Pergamon

European Journal of Cancer, Vol. 35, No. 7, pp. 1102–1108, 1999

Printed in Great Britain
0959-8049/99/$ - see front matter

PII: S0959-8049(99)00053-2

Original Paper

Cerebral Blood Flow and Glucose Metabolism in Long-term Survivors of Childhood Acute Lymphoblastic Leukaemia

M. Kähkönen,[1,2] A. Harila-Saari,[8] L. Metsähonkala,[1,2] T. Korhonen,[3] M.-K. Norvasuo-Heilä,[4] T. Utriainen,[7] A. Ahonen,[9] J. Bergman,[5] T.T. Salmi[2] and H. Minn[6]

[1]Turku PET Centre and [2]Departments of Paediatrics, [3]Child Psychiatry, [4]Neurology, [5]Radiochemistry Laboratory, [6]Radiation and Oncology, University of Turku, PO Box 52, FIN-20520 Turku; [7]Department of Medicine, University of Helsinki, Helsinki; [8]Departments of Paediatrics, and [9]Clinical Chemistry, Division of Nuclear Medicine, University of Oulu, Oulu, Finland

Central nervous system treatment for childhood acute lymphoblastic leukaemia (ALL) has been reported to cause changes in cerebral blood flow and glucose metabolism. Little is known about the association of these functional changes with neuropsychological defects and structural changes. The aim of the present study was to assess the relationship between changes in regional cerebral blood flow and glucose utilisation in long-term survivors of ALL, and the association of these functional abnormalities with neurocognitive and structural defects. 8 survivors of childhood ALL were studied with single photon emission tomography (SPECT) using Tc99m-ethyl cysteinate dimer (ECD) as tracer and with positron emission tomography (PET) using ^{18}F-fluorodeoxyglucose (FDG) as tracer. 8 healthy controls also underwent FDG-PET. All subjects also underwent magnetic resonance imaging and neuropsychological assessment 5 years after cessation of the therapy. Focal cerebral blood flow abnormalities were found in ECD-SPECT in 5 of the 8 survivors. Glucose utilisation appeared normal in the corresponding regions. However, glucose utilisation was decreased in thalamus and cerebellum in the survivors of ALL as compared with healthy controls. 3 patients had severe and 5 patients mild neurocognitive difficulties. The changes in cerebral blood flow and FDG uptake did not correspond neuroanatomically with the neurocognitive defects. Focal defects in cerebral blood flow in long-term survivors of ALL are not associated with changes in local cerebral glucose utilisation. Neurocognitive difficulties are not consistently associated with either changes in cerebral blood flow or with decreased glucose utilisation. Therefore, based on the present set of studies FDG-PET and ECD-SPECT cannot yet be recommended for the evaluation of long-term neurocognitive defects associated with treatment of ALL. © **1999 Elsevier Science Ltd. All rights reserved.**

Key words: leukemia, late effect, FDG-PET, ECD-SPECT, child
Eur J Cancer, Vol. 35, No. 7, pp. 1102–1108, 1999

INTRODUCTION

PROPHYLACTIC TREATMENT of the central nervous system (CNS) with combined cranial irradiation therapy (CRT) and systemic plus intrathecal methotrexate (MTX) or MTX alone has dramatically reduced the incidence of CNS relapses and improved the survival of children with acute lymphoblastic leukaemia (ALL). However, CRT and/or MTX may be associated with morphological changes in the brain [1, 2] and with cognitive decline [3]. Even low doses of cranial irradiation (18 Gy) can have harmful effects on neurocognitive function in ALL long-term survivors [4, 5].

Histopathological studies have shown that at least three different types of morphological CNS defects can be found in ALL long-term survivors: subacute leucoencephalopathy, mineralising micro-angiopathy and cortical atrophy [1].

Correspondence to M. Kähkönen, e-mail: meri.kahkonen@pet.tyks.fi
Received 29 Oct. 1998; revised 25 Jan. 1999; accepted 3 Feb. 1999.

These morphological changes have been detected even in asymptomatic long-term survivors [1]. The neuropsychological impairment associated with CRT may result from vascular lesions, demyelination, or both [6]. Demyelination is thought to occur due to primary demineralisation of myelin or secondary to vascular insufficiency [6]. The latter might be due to damage to endothelial cells in capillaries, sinusoids and small arterioles, which could reduce regional CNS perfusion [7].

Changes in cerebral blood flow as measured with single photon emission tomography (SPECT) have recently been reported in patients with ALL during, immediately after and 5 years after cessation of therapy [8–10]. The perfusion defects occurred most often in chemotherapy-treated patients at the end of therapy and in irradiated patients 5 years after cessation of therapy. This is in accordance with the finding that high-dose MTX may result in severe but at least partly reversible cerebral perfusion defects [8], whilst CRT-induced vascular injury is delayed [7]. Thus, a sufficiently long follow-up time after irradiation is necessary to demonstrate perfusion defects induced by CRT.

Decreased rates of regional cerebral glucose utilisation have been found with ^{18}F-fluoro-deoxyglucose positron emission tomography (FDG-PET) in long-term survivors of childhood ALL [11, 12]. Studies with 2-[^{14}C]-deoxyglucose and autoradiography in rats [13] and FDG-PET in patients with brain tumours [14] have suggested that the decreased rate of glucose utilisation is related to CRT-induced cerebral dysfunction. However, a direct association between PET findings and neuropsychological impairment has not been demonstrated.

The present study was undertaken to evaluate whether brain perfusion defects of ALL long-term survivors are linked to altered cerebral glucose utilisation and, more importantly, whether metabolic and/or perfusion defects are associated with neurocognitive impairment. For this purpose, we studied the distribution of the cerebral blood flow with Tc99m ethyl cysteinate dimer (ECD)-SPECT, and regional cerebral glucose utilisation with FDG-PET, and performed neurocognitive assessment in 8 long-term survivors of childhood ALL.

PATIENTS AND METHODS

Patients and control subjects

8 long-term survivors of childhood ALL participated in the study. The patients were studied 5 years after cessation of the therapy for ALL, and they were all on continuous complete first remission. The diagnosis of ALL was made over a time period from May 1986 to November 1988 and all patients were treated at the Department of Paediatrics of Oulu University Hospital. None of the patients had CNS disease at the time of primary diagnosis. Characteristics of the subjects are shown in Table 1. The mean age of the patients at diagnosis was 6.4 years and at the time of the present studies 14.0 years.

The patients were treated according to the Nordic Society for Paediatric Haematology and Oncology (NOPHO) protocols for standard (SR) ($n = 3$), intermediate (IR) ($n = 2$) and high risk (HR) ($n = 3$) ALL. Details of the prophylactic treatment of CNS are shown in Table 1. The treatment protocols have previously been reported in detail [15–17].

7 children had developed normally before their disease, and 1 (no. 6) had had slight delay in verbal and motor development. Pretreatment baseline tests for cognitive skills were not done.

To establish normal values for cerebral glucose utilisation we studied a group of 8 healthy, young male volunteers with FDG-PET. Their mean age was 25.4 (24.3–26.8) years.

Ethics

The study was reviewed and approved by the Joint Committee on Ethics of the Turku University Central Hospital and the University of Turku and by the Ethical Committee of the Medical Faculty of the University of Oulu. The nature, purpose and potential risks of the study were explained to all subjects and/or their legal guardians before they gave their informed written consent.

Study design

ECD-SPECT and MRI were performed on the same day at Oulu University Central Hospital, and FDG-PET studies were performed within 18 months after SPECT and MRI at the Turku PET Centre and Turku University Central Hospital. In addition, each patient went through a comprehensive neurocognitive assessment temporally close to the PET study.

PET imaging

The PET studies were performed under postabsorptive conditions in a quiet and dimmed room with an eight-ring ECAT 931/08-tomograph (Siemens/CTI Corp., Knoxville, Tennesee, U.S.A.). The scanner has an axial resolution of 6.7 mm and in-plane resolution of 6.5 mm [18]. The entire brain could be scanned with an axial field of view of 11.8 cm.

Table 1. *Characteristics of the ALL long-term survivors*

Patient no.	Sex	Age at diagnosis (yr)	Treatment protocol	CRT (Gy)	Number of MTX i.t. injections	Dose of MTX i.v. injections (g/m^2)	Age at study (yr)	Abnormal brain MRI findings
1	M	5.5	SR84		7	3×1	13.6	None
2	F	5.3	SR86		13	8×1	13.3	None
3	F	3.1	SR86		13	8×1	11.0	None
4	F	9.3	IM86	18	9	4×0.5	17.3	None
5	F	4.1	IM86	18	9	4×0.5	12.0	None
6	F	2.1	HR86	24	11	6×0.5	10.1	Enlarged left ventricle
7	M	15.4	HR86	24	11	6×0.5	24.0	None
8	F	6.3	HR86	24	11	6×0.5	14.3	White matter change

SR84 is a treatment protocol introduced in 1984 for standard risk ALL according to the Nordic Society for Paediatric Haematology and Oncology (NOPHO). SR86, IM86 and HR86 are the treatment protocols for standard risk, intermediate risk and high risk ALL, respectively, introduced in 1986 by NOPHO. i.t., intrathecal; i.v., intravenous; CRT, cranial irradiation therapy; MRI, magnetic resonance imaging.

An individually shaped light foam rubber holder was used for fixation of the head.

Production of [^{18}F]FDG. The 2-[^{18}F]fluoro-2-deoxy-D-glucose synthesis was a modification of the method reported by Hamacher and colleagues [19]. The radiochemical purity always exceeded 99%.

Blood sampling, image acquisition and processing. Before start of data acquisition, two venous cannulas were inserted, one antecubitally for injection of FDG and another in the pre-heated contralateral forearm for blood sampling.

Subsequently, a 10 min transmission scan for correction of photon attenuation was performed with a removable ring source containing ^{68}Ge. Following a bolus injection of FDG (2.8 MBq/kg), dynamic emission scan was acquired for 55 min (4×30 sec, 3×60 sec, 10×300 sec frames). To measure input function of the tracer, a total of 20 blood samples were withdrawn from the forearm vein during the acquisition. All data were corrected for decay and measured photon attenuation. Dynamic scans were reconstructed pixel by pixel into a 128×128 matrix with a Bayesian iterative reconstruction algorithm using median root prior (the MRP method) [20] with 150 iterations and the Bayesian coefficient 0.3. The final spatial resolution in reconstructed images was 8.0 mm.

Calculation of regional cerebral metabolic rate for glucose (rCMRGlc). In addition to visual analysis by two independent observers, a quantitative analysis was performed. For determination of the regional cerebral metabolic rate for glucose, a three compartmental model of [^{18}F]FDG kinetics was used as previously described [21]. Plasma and tissue activity curves were analysed graphically to calculate a rate constant (K_i) for the fractional rate of tracer transport and phosporylation [22]. The rCMRGlc was obtained as follows:

$$\text{rCMRGlc} = K_i \times \text{Glc}_p/\text{LC}$$

where Glc_p denotes the average plasma glucose concentration during the acquisition, and LC denotes differences in the transport and phosporylation of FDG and glucose. The value of LC was assumed to be 0.81 as recently described in humans [23].

Regions of interest. Individually shaped, multi-angular regions of interest (ROIs) were outlined on cortical and subcortical areas according to guidance of brain atlas [24]. ROIs were drawn on frontal, temporal, parietal and occipital cortex and striatum, cerebellum and white matrix in a manner that enabled the covering of the whole cortex in each plane. The total number of ROIs in each brain varied between 60 and 75. Asymmetry between the hemispheres on cortical and subcortical regions in percentages was calculated as follows:

$$\text{Asymmetry} = (\text{ROI}_{dx} - \text{ROI}_{sin})/(\text{ROI}_{dx} + \text{ROI}_{sin}) \times 100\%$$

where ROI stands for mean radioactivity concentration within a ROI, and *dx* and *sin* for right and left hemispheres, respectively. Asymmetries were considered to be abnormal if they exceeded 2 standard deviations (S.D.s) of the mean asymmetries of the control subjects.

Measurement of cerebral blood flow with SPECT

Brain SPECT was performed using Technetium-99m ethyl cysteinate dimer ECD as the tracer, which was administered according to the patients' body surface area as previously described [25]. To achieve an attenuated sensory state, the eyes were covered with patches and the subject lay supine with the head secured to the bed in a dimmed quiet room for 10 min prior to the intravenous (i.v.) injection of the tracer. The eyes remained covered during the injection and for approximately 5 min afterwards. SPECT was performed 15–60 min after the i.v. administration of the tracer. The images were acquired with a double-head rotating gamma camera (ADAC Vertex, ADAC Laboratories, Milpitas, California, U.S.A.) equipped with a fanbeam collimator.

Sixty-four projections were obtained in a 128×128 matrix, which were acquired over a 360° circular orbit with a radius of about 14 cm, each view containing an average of 65 kilocounts. The filtered backprojection algorithm used a Butterworth filter with a cut-off of 0.22 of Nygwist frequency and an order of 5.0. No attenuation correction was used. Orbitomeatal line-oriented transverse, sagittal and coronal sections were processed. Two slices were then summed to the total slice thickness of 9.4 mm for visual interpretation and semiquantitative analysis.

Tracer distribution in the right and left hemispheres was evaluated both visually and semiquantitatively. For semiquantitative analysis two-pixel-wide strip was placed over the transversal slice (occasionally coronal). Asymmetry between the hemispheres in percentages was calculated as follows:

$$\text{Asymmetry} = (\text{ROI}_{max} - \text{ROI}_{min})/\text{ROI}_{max} \times 100\%$$

where ROI stands for count rate within a ROI, and min and max for the pathological area defined in visual analysis and the symmetrical normal area of the other hemisphere, respectively. The images were evaluated with knowledge of the nature of the disorder, but totally blinded for the treatment. The brain SPECT was classified as abnormal if the SPECT scans were visually interpreted as definitely abnormal (a clearly visible asymmetry in the tracer accumulation between the hemispheres was observed in at least two consecutive slices) and hemispheric asymmetry in semiquantification was equal to or more than 10%.

MRI

The patients had undergone MRI studies of the brain as a part of their neurological follow-up [26]. MRI was performed with a 1.0 T scanner (Magnetom, Siemens, Erlangen, Germany). T2-weighted axial and coronal (turbo spin echo or fast spin echo) images (TR 3500, TE 14–15, 93–98, 1 excitation, 5 mm slice, 192 – 224×256 matrix, 23 cm field of view), together with sagittal T1-weighted images (TR 400–570, TE 9–15, 2 excitations, 3 or 5 mm slice, 176 – 224×256 matrix, 23–24 cm field of view), were obtained. The MRIs were reviewed independently by two radiologists.

Neurocognitive assessment

The neurocognitive functions were assessed in seven areas: verbal comprehension, perceptual organisation, freedom from distractibility, fine motor, visual-motor integration, memory and learning, and executive functions (Table 2). A descriptive case approach was used in reporting the results. When possible, standardised norms of tests were applied in the following manner: a test result poorer than the mean—2 S.D. was supposed to indicate a clear, indisputable difficulty labelled as 'severe', while a test score better than the mean—2 S.D., but poorer than the mean—1 S.D. was supposed to

express an equivocal problem labeled as 'mild'. In the Rey's Complex Figures test, for which there were no standardised norms available, the decision on a label was provided by a consensus of the rating given by two experienced clinical neuropsychologists. The final score for each of the neurocognitive functions was decided following the poorest test result of the subject in the functional area.

Statistical methods

Student's unpaired two-tailed *t*-test was used to compare the means of rCMRGlc of the ALL long-term survivors and the control subjects. All data are expressed as mean ± S.D. *P* values less than 0.05 were considered statistically significant. The hemispheric asymmetries of rCMRGlc in the control subjects were calculated to represent normal ranges of asymmetry. The regional asymmetries of CMRGlc between right and left hemispheres were calculated separately in each plane. The regional asymmetry was considered to be abnormal if it exceeded 2 S.D. of the mean asymmetry of the control subjects in two or more consecutive planes. The 95% confidence intervals were calculated to confirm the upper limits considered as normal variability of asymmetry in each cerebral region.

RESULTS

Cerebral glucose utilisation

Mean concentrations of blood glucose during the PET study were 5.0 mmol/l (range 4.3–6.1 mmol/l) in the patients and 5.4 mmol/l (4.9–6.2 mmol/l) in the control subjects. Blood glucose concentration remained stable in each subject during the scan acquisition time. The rCMRGlc of cortical and subcortical areas and cerebellum are shown in Table 3. Regional glucose utilisation was significantly lower in the thalamus in the patients as compared with the control subjects ($P = 0.04$). There was no difference or tendency to any distinct pattern between the rCMRGlc of the left and right side of thalamus. In addition, the rCMRGlc in the cerebellum was lower in the patients as compared with the control subjects ($P = 0.05$).

In FDG-PET studies, a range of normal hemispheric asymmetry was considered to be lower than or equal to the measured mean + 2 S.D. of the asymmetry of glucose metabolic rates in the control subjects. The normal ranges for asymmetry were 0–6.1% in frontal, 0–9.5% in parietal, 0–5.2% in temporal and 0–11.6% in occipital cortical regions. The respective ranges were 0–5.5% in striatum, 0–5.7% in cerebellum and 0–5.8% in white matrix. Among the patients, asymmetries of rCMRGlc were within the range considered as normal variability in each area (data not shown).

Table 2. The neurocognitive test methods [Ref.]

Verbal comprehension	Subtest similarities and comprehension from Wechsler Intelligence scale for children—revised [35] and Wechsler Adult intelligence scale—revised [36]
Perceptual organisation	Subtest block design and object assembly from Wechsler [35, 36]
Freedom from distractibility	Subtests digit span and coding from Wechsler [35, 36]
Fine motor	The Purdue pegboard test [37]
Visual-motor integration	Rey's complex figures test [38], the developmental test of Visual-motor integration [39]
Memory and learning	Selective reminding test (verbal and visual forms) [40, 41]
Executive performance	Trail making B [38]

Cerebral blood flow

The localisations of cerebral perfusion defects as assessed by ECD-SPECT are shown in Table 4. The cutoff point for hemispheric asymmetry was $\geq 10\%$ [29]. Perfusion defects were observed in various cerebral areas and cerebellum without any distinct pattern. Cerebral blood flow was decreased in two areas of the brain in 2 subjects, and in a single area in 3 subjects. In these patients the hemispheric asymmetry ranged from 10 to 45%. 3 patients had no abnormalities in their perfusion scans. One of these 3 had, however, severe deficits in neurocognitive functioning (see below).

Structural lesions

2 patients had abnormal findings on brain MRI (Table 1).

Neurocognitive defects

The findings of the neurocognitive assessment are shown in detail in Table 4. 3 patients had severe neurocognitive defects and 5 other patients showed mild neurocognitive defects. The neurocognitive defects seemed to be linked to a general slow rate of cognitive processing. In 1 patient (no. 6) the impact of slight pretreatment delay in development on current neurocognitive defects cannot be excluded.

Co-localisation of blood flow, glucose utilisation, structural lesions and neurocognitive defects

In visual and quantitative analysis, glucose utilisation appeared normal in all of the areas where perfusion defects were observed (Figure 1). Likewise, the abnormal structural findings in MRI were neither in the same areas as the perfusion defects nor in the areas of decreased glucose utilisation. Focal defects in certain brain regions are often associated with a specific type of neurocognitive impairment. However, the abnormal findings in the neurocognitive assessment could not be directly attributed to the observed areas of decreased glucose utilisation, i.e. thalamus and cerebellum. In only 3 patients (nos 4, 6, 7) were the defects in blood flow in regions that neuro-anatomically corresponded well with the neurocognitive defects.

Table 3. Regional glucose utilisation in ALL long-term survivors and control subjects

Region	Regional glucose utilisation (μmol/min/100 g)	
	ALL survivors	Control subjects
Frontal cortex	37.1 ± 6.7	34.4 ± 3.5
Parietal cortex	32.7 ± 5.2	31.6 ± 4.8
Temporal cortex	32.4 ± 5.1	32.4 ± 3.6
Occipital cortex	30.6 ± 3.2	29.6 ± 3.8
Cerebellum	24.1 ± 3.9	28.0 ± 3.2*
Striatum	34.1 ± 4.4	35.0 ± 3.7
Thalamus	29.5 ± 5.6	35.1 ± 3.7†
White matrix	20.9 ± 3.7	21.5 ± 1.9

Data are mean ± S.D. (standard deviation). *$P = 0.05$. †$P = 0.04$.

Table 4. Findings of ECD-SPECT and neurocognitive assessment in ALL long-term survivors

Patient no.	ECD-SPECT Localisation of the defect	ECD-SPECT Per cent of the difference	Neurocognitive impairment (mild = below 1 S.D., severe = below 2 S.D.)
1	Left posteroparieto-occipital	17	Mild in freedom from distractibility
2	None	ns	Mild in memory functions
3	Right occipito-cerebellar	12	Severe in executive functions
4	Left anterofrontal and cerebellum	45	Mild in fine motor functions
5	None	ns	Severe in memory and learning functions, mild in perceptual organisation, freedom from distractibility and visual-motor integration
6	Right basofrontal and left temporal	10	Severe in executive functions, mild in freedom from distractibility
7	Left anterotemporal	15	Mild in fine motor and learning and memory functions
8	None	ns	Mild in fine motor

ECD-SPECT, ethyl cysteinate dimer-single photon emission tomography; ns, not significant; S.D., standard deviation.

DISCUSSION

The progression of ALL has improved greatly during the last decades and it is of increasing importance to recognise long-term side-effects caused by treatment. The cognitive defects associated with prophylactic treatment of neuroleukaemia can be specifically hazardous, since neurocognitive impairment inevitably results in decreased functioning in social and professional life. Modern functional neuro-imaging methods are attractive tools for assessment of cognitive defects owing to the non-invasiveness and lack of subjectivity inherent to the techniques. We used SPECT and PET to assess cerebral blood flow and metabolism in ALL long-term survivors and found focal defects in blood flow in different areas of the brain in 5 out of 8 study subjects. Despite 10–45% lower rates of regional blood flow, we could not observe any significant changes in rCMRGlc in the corresponding brain regions.

Focal defects in certain brain regions are often associated with a specific type of neurocognitive impairment. In the present study, regional perfusion defects corresponded neuro-anatomically well with the neurocognitive defects in 3 patients, while 1 patient with severe neurocognitive difficulties had no perfusion defect, and 2 patients presented with only a minor perfusion defect (10–12%) in non-related regions. Thus, our results indicate that neurocognitive defects are not necessarily spatially related to perfusion defects.

We could not observe any abnormalities in cortical glucose utilisation in patients with defects in cerebral blood flow and/or neurocognitive defects. Instead, we found that regional glucose utilisation was lower in the thalamus and in the cerebellum in the patients in comparison to the control subjects. Our finding is consistent with previous data presented by Phillips and colleagues which demonstrated decreased rCMRGlc in the thalamus in ALL long-term survivors [11]. In our earlier study [12], the patients with neurocognitive difficulties were found to have globally decreased cortical glucose utilisation in comparison with patients with no neurocognitive difficulties. In the present study, with more accurate regional analysis and a healthy control population, neither regional cortical lesions nor overt cortical decreased glucose uptake were noticed.

The interval between SPECT and PET studies was several months in some cases. This is, however, a short interval in comparison with the time elapsed from the cessation of treatment which had been given 5 years earlier. Delayed vascular injury develops up to several years after treatment and is

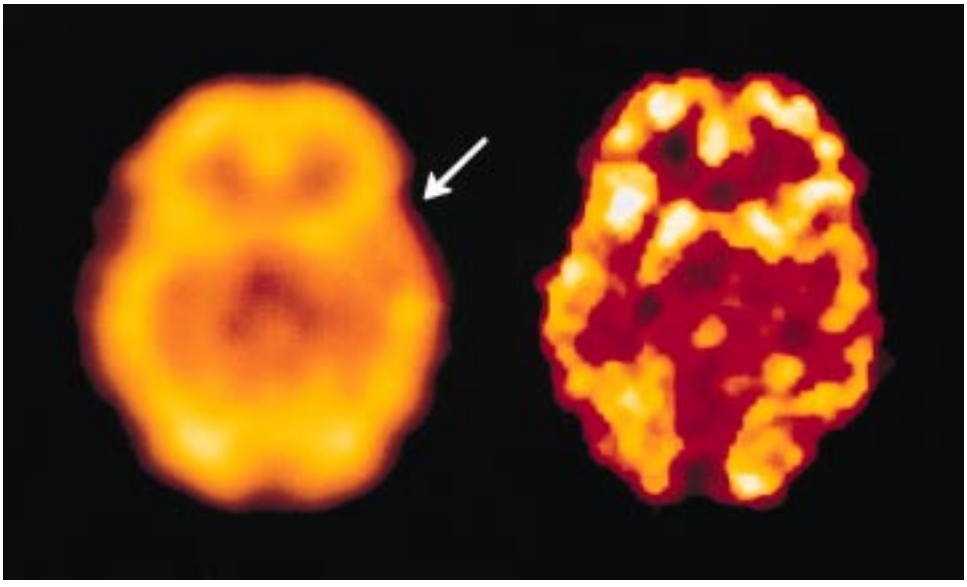

Figure 1. Example of ECD-SPECT (a) and FDG-PET (b) images depicting a 15% perfusion defect in the anterotemporal cortex (arrow), and a symmetrical accumulation of FDG in the cortex at the same level.

irreversible. Thus, the perfusion defects seen in the SPECT study are likely to be permanent and would also exist at the time of the PET study. Therefore, it is evident that the corresponding cerebral glucose utilisation was unchanged in our patients despite mild to moderate defects in cerebral blood flow.

Cerebral glucose utilisation has been suggested to be age-dependent in the PET study by Chugani and colleagues [27]. These authors suggested that rCMRGlc values reach a peak at the age of 8 years and decline slowly after that to values observed in adults. Age-dependency might seriously affect intersubject comparison of absolute rCMRGlc values for children, but it is of concern that children in the study by Chugani and colleagues were suspected of having neurological disease and may thus, not reflect a normal population in an appropriate manner. We found no age-dependency in the rCMRGlc values in our adolescent patients. The lower CMRGlc in the thalamus and cerebellum would be even more significant if age-dependency in the rCMRGlc had been noticed. In addition, the interhemispheric asymmetries of glucose utilisation, which are not supposed to be affected by age, were also compared between the controls and the patients.

Owing to FDG uptake of the white matter is lower than that in the cortex and the basal ganglia, delineation of the border between grey and white matter in PET images needs special attention. The grey matter of the adolescent cerebral cortex is only 5–7 mm thick, thus representing a potential source of error in calculation of the rCMRGlc caused by problems associated with tissue heterogeneity and partial volume effects. The possibility of distinguishing white matter from cortex, and vice versa, was facilitated in our study by using a recently developed iterative reconstruction method utilising the median root prior (MRP) [20]. The MRP method enhances image resolution by improving the signal-to-noise ratio thus minimising the effect of heterogeneity. Therefore, it enables more accurate quantitation of rCMRGlc in small brain areas.

Perfusion imaging of the brain with SPECT has specific limitations which are inherent in the sensitivity and resolution of the system. Firstly, the lack of normal reference values has until now restricted evaluation of perfusion defects especially in children and young adults. This problem has recently been addressed by Barthel and colleagues [28] and Schiepers and colleagues [29] who have reported normal values of ECD-SPECT tracer distribution in pre-school and school age children and adults. A second limitation is the insensitivity of SPECT to detect symmetric changes in very small areas such as thalamus or other structures in the basal ganglia. It is evident that perfusion defects in these small areas may be overlooked with SPECT, contrary to PET, which can be used for evaluation of metabolism in the thalamus as shown by our study.

In the present study, structural changes were found in only 2 patients using MRI. MRI findings did not correspond to either defects in blood flow or glucose utilisation, or to neurocognitive defects. These findings are consistent with the previous data demonstrating no association between structural changes using MRI and neuropsychological defects or cerebral blood flow using SPECT [9, 30]. Previous studies using cranial CT have shown focal calcifications in basal ganglia which are associated with impaired verbal memory and learning [31], and lower intelligence quotient (IQ) [32]. MRI has been shown to be less sensitive to detect calcifications than CT [32, 33]. The decrease in thalamic glucose utilisation reflects functional changes in the area of the basal ganglia, which can be visualised in MRI only if they lead to structural damage.

In this study, neither irreversible vascular damage nor disruption of cellular glucose utilisation could adequately explain the neurocognitive defect. The alternative explanation is that CRT results in a disturbance of myelin synthesis which could then impair neuropsychological functioning [6]. During the first 4 years of life, brain development is characterised by rapid synthesis of myelin. When CNS therapy is given in early childhood during the particularly vulnerable period of CNS development, interruption of myelin synthesis could result in, for example, impaired perceptual processing [6]. In our study, 3 patients had severe and the remaining 5 mild neurocognitive impairment, either in some executive functions, or in memory and verbal learning functions (Table 3). Interestingly, the 3 patients with severe impairment were the youngest subjects in our study group at the time of CNS treatment (age 2.1–4.0 years at diagnosis). This finding is in agreement with a previous meta-analysis on ALL long-term survivors, which implied that children irradiated before the age of 4 years are at increased risk of severe IQ decrements after CRT [4].

In addition, as neurons, axons and supportive glial cells of the CNS display a high rate of metabolic activity, they are vulnerable to even brief disruptions of energy supply [34]. Even transient perfusion defects might, therefore, result in irreversible damage to myelinated axons and their neural connections, which are critical for normal signal transmission. The transient perfusion defects and their effect on signal transmission cannot be measured by the methods currently used. Thalamic glucose hypometabolism could be connected to abnormalities in neural connections. However, these abnormalities do not seem to cause a change in the overall cortical glucose metabolism. In addition, the generalised slow rate of cognitive processing in our patients might, in particular, reflect injury to these connections.

In summary, focal changes of cerebral perfusion seen in ALL long-term survivors are not accompanied with defects in glucose metabolism in the corresponding regions. Furthermore, neurocognitive difficulties do not seem to be clearly associated with changes in cerebral perfusion or with decreased glucose utilisation. Our findings, therefore, suggest that mechanisms other than irreversible vascular defects may also be important for changes in cognitive function. Although our study population was somewhat heterogenous as regards treatment modalities used, age of the patients during ALL treatment and age of the subjects during the study, it seems that functional imaging methods, specifically FDG-PET and ECD-SPECT, are of limited value in the evaluation of ALL long-term survivors with clinical signs of neurological defects. Therefore, FDG-PET and ECD-SPECT cannot yet be recommended for the routine follow-up of these subjects.

1. Price RA, Jamieson PA. The central nervous system in childhood leukemia. II. Subacute leukoencephalopathy. *Cancer* 1975, **35**, 306–318.
2. Bleyer WA. Neurologic sequelae of methotrexate and ionizing radiation: a new classification. *Cancer Treat Rep* 1981, **65**(Suppl. 1), 89–98.
3. Meadows AT, Gordon J, Massari DJ, Littman P, Fergusson J, Moss K. Declines in IQ scores and cognitive dysfunctions in children with acute lymphocytic leukaemia treated with cranial irradiation. *Lancet* 1981, **2**, 1015–1018.

4. Jankovic M, Brouwers P, Valsecchi MG, *et al.* Association of 1800 cGy cranial irradiation with intellectual function in children with acute lymphoblastic leukaemia. ISPACC. International Study Group on Psychosocial Aspects of Childhood Cancer. *Lancet* 1994, **344**, 224–227.
5. Smibert E, Anderson V, Godber T, Ekert H. Risk factors for intellectual and educational sequelae of cranial irradiation in childhood acute lymphoblastic leukaemia. *Br J Cancer* 1996, **73**, 825–830.
6. Dowell Jr RE, Copeland DR. Cerebral pathology and neuropsychological effects. Differential effects of cranial radiation as a function of age. *Am J Pediatr Hematol Oncol* 1987, **9**, 68–72.
7. Valk PE, Dillon WP. Radiation injury of the brain. *Am J Neuroradiol* 1991, **12**, 45–62.
8. Osterlundh G, Bjure J, Lannering B, Kjellmer I, Uvebrant P, Marky I. Studies of cerebral blood flow in children with acute lymphoblastic leukemia: case reports of six children treated with methotrexate examined by single photon emission computed tomography. *J Pediatr Hematol Oncol* 1997, **19**, 28–34.
9. Harila-Saari AH, Ahonen AK, Vainionpää LK, *et al.* Brain perfusion after treatment of childhood acute lymphoblastic leukemia. *J Nucl Med* 1997, **38**, 82–88.
10. Harila-Saari AH, Lanning BM, Ahonen AK, Vainionpää LK. Brain blood flow changes in 99mTc-ECD SPECT five years after cessation of therapy for childhood ALL. *NOPHO 16th Annual Meeting* 1998, **45** (Abstract).
11. Phillips PC, Moeller JR, Sidtis JJ, *et al.* Abnormal cerebral glucose metabolism in long-term survivors of childhood acute lymphocytic leukemia. *Ann Neurol* 1991, **29**, 263–271.
12. Suhonen-Polvi H, Salmi TT, Korhonen T, *et al.* Cerebral glucose utilization measured with positron emission tomography (PET) as an index for neurological functioning in long-term survivors of childhood acute lymphoblastic leukemia (ALL). *Int J Pediatr Hematol Oncol* 1995, **2**, 63–71.
13. Ito M, Patronas NJ, Di Chiro G, Mansi L, Kennedy C. Effect of moderate level x-radiation to brain on cerebral glucose utilization. *J Comput Assist Tomogr* 1986, **10**, 584–588.
14. Mineura K, Yasuda T, Kowada M, Ogawa T, Shishido F, Uemura K. Positron emission tomographic evaluation of radiochemotherapeutic effect on regional cerebral hemocirculation and metabolism in patients with gliomas. *J Neurooncol* 1987, **5**, 277–285.
15. Gustafsson G, Garwicz S, Hertz H, *et al.* A population-based study of childhood acute lymphoblastic leukemia diagnosed from July 1981 through June 1985 in the five Nordic countries. Incidence, patient characteristics and treatment results. *Acta Paediatr Scand* 1987, **76**, 781–788.
16. Gustafsson G, Berglund G, Garwicz S, *et al.* A population-based study of children with standard risk acute lymphoblastic leukemia in the five Nordic countries. A follow-up of 230 patients. *Acta Paediatr Scand* 1989, **78**, 104–109.
17. Riehm H, Reiter A, Schrappe M, *et al.* Corticosteroid-dependent reduction of leukocyte count in blood as a prognostic factor in acute lymphoblastic leukemia in childhood (therapy study ALL-BFM 83). *Klin Padiatr* 1987, **199**, 151–160.
18. Spinks TJ, Jones T, Gilardi MC, Heather JD. Physical performance of the latest generation of commercial positron scanner. *IEEE T Nucl Sci* 1988, **35**, 721–725.
19. Hamacher K, Coenen HH, Stocklin G. Efficient stereospecific synthesis of no-carrier-added 2-(18F)-fluoro-2-deoxy-D-glucose using aminopolyether supported nucleophilic substitution. *J Nucl Med* 1986, **27**, 235–238.
20. Alenius S, Ruotsalainen U. Bayesian image reconstruction for emission tomography based on median root prior. *Eur J Nucl Med* 1997, **24**, 258–265.
21. Phelps ME, Huang SC, Hoffman EJ, Selin C, Sokoloff L, Kuhl DE. Tomographic measurement of local cerebral glucose metabolic rate in humans with (F-18)2-fluoro-2-deoxy-D-glucose: Validation of method. *Ann Neurol* 1979, **6**, 371–388.
22. Patlak CS, Blasberg RG. Graphical evaluation of blood-to-brain transfer constants from multiple-time uptake data. Generalizations. *J Cereb Blood Flow Metab* 1985, **5**, 584–590.
23. Hasselbalch SG, Madsen PL, Knudsen GM, Holm S, Paulson OB. Calculation of the FDG lumped constant by simultaneous measurements of global glucose and FDG metabolism in humans. *J Cereb Blood Flow Metab* 1998, **18**, 154–160.
24. Aquilonius S-M, Eckernäs S-Å. *A Colour Atlas of the Human Brain*. New York, Raven Press, 1980.
25. Piepsz A, Hahn K, Roca I, *et al.* A radiopharmaceuticals schedule for imaging in paediatrics. Paediatric Task Group European Association Nuclear Medicine. *Eur J Nucl Med* 1990, **17**, 127–129.
26. Harila-Saari AH, Pääkkö EL, Vainionpää LK, Pyhtinen J, Lanning BM. A longitudinal magnetic resonance imaging study of the brain in survivors of childhood acute lymphoblastic leukemia. *Cancer* 1998, **83**, 2608–2617.
27. Chugani HT, Phelps ME, Mazziotta JC. Positron emission tomography study of human brain functional development. *Ann Neurol* 1987, **22**, 487–497.
28. Barthel H, Wiener M, Dannenberg C, Bettin S, Sattler B, Knapp WH. Age-specific cerebral perfusion in 4- to 15-year-old children: a high-resolution brain SPET study using 99mTc-ECD. *Eur J Nucl Med* 1997, **24**, 1245–1252.
29. Schiepers C, Verbruggen A, Casaer P, De Roo M. Normal brain perfusion pattern of technetium-99m-ethylcysteinate dimer in children. *J Nucl Med* 1997, **38**, 1115–1120.
30. Kingma A, Mooyaart EL, Kamps WA, Nieuwenhuizen P, Wilmink JT. Magnetic resonance imaging of the brain and neuropsychological evaluation in children treated for acute lymphoblastic leukemia at a young age. *Am J Pediatr Hematol Oncol* 1993, **15**, 231–238.
31. Brouwers P, Poplack D. Memory and learning sequelae in long-term survivors of acute lymphoblastic leukemia: association with attention deficits. *Am J Pediatr Hematol Oncol* 1990, **12**, 174–181.
32. Mulhern RK, Kovnar E, Langston J, *et al.* Long-term survivors of leukemia treated in infancy: factors associated with neuropsychologic status. *J Clin Oncol* 1992, **10**, 1095–1102.
33. Pääkkö E, Talvensaari K, Pyhtinen J, Lanning M. Late cranial MRI after cranial irradiation in survivors of childhood cancer. *Neuroradiology* 1994, **36**, 652–655.
34. Stys PK. Anoxic and ischemic injury of myelinated axons in CNS white matter: from mechanistic concepts to therapeutics. *J Cereb Blood Flow Metab* 1998, **18**, 2–25.
35. Wechsler D. *Wechsler Intelligence Scale for Children—Revised*. Helsinki, Psykologien Kustannus Oy, 1984.
36. Wechsler D. *Wechsler Adult Intelligence Scale—Revised*. Helsinki, Psykologien Kustannus Oy, 1992.
37. Tiffin J. *Examiner's Manual*. Chicago, Science Research Associates, 1968.
38. Lezak M. *Neuropsychological Assessment*. New York, Oxford University Press, 1983.
39. Beery KE. The VMI. Developmental test of visual-motor integration. In *Administration, Scoring, and Teaching Manual*. Cleveland, Modern Curriculum Press, 1989.
40. Buschke. Component of verbal learning in children: analysis by selective reminding. *J. Exp. Child Psyc.* 1974, **18**, 488–496.
41. Fletcher JM. Memory for verbal and nonverbal stimuli in learning disability subgroups: analysis by selective reminding. *J Exp Child Psyc* 1985, **40**, 244–259.